DOI: 10.1002/ejic.200500654

Preparation of Semiconductor/Polymer Coaxial Nanocables by a Facile Solution Process

Shenglin Xiong,[b] Linfeng Fei,[a] Zhenghua Wang,[b] Hong Yang Zhou,[b] Weizhi Wang,[b] and Yitai Qian*[a,b]

Keywords: Hydrothermal synthesis / Nanostructures / Photoluminescence / Semiconductors / Tellurium

We report on the preparation of ultralong semiconductor tellurium/cross-linked PVA coaxial nanocables with a core 20–30 nm in diameter and a surrounding sheath about 5–20 nm in thickness by a simple hydrothermal process. The length of these nanocables can be up to 500–800 μm. In the present synthesis PVA was used as the reducing agent to react with Na_2TeO_3, and it also serves as the capping reagent and the source of the sheaths. The synergistic effects of the interaction of cross-linked PVA with the tellurium nanowires could play an important role in the formation of the morphology of the resulting products.

Introduction

Nanomaterials with a core/sheath structure as another new type of one-dimensional nanostructures have, in recent years, been attracting more and more interest since these heterostructured nanostructures are constructed of cores and shells of different chemical compositions, which could further improve their functions by the preparation of the core and sheath from different materials.[1–5] In particular, coaxial nanocables with a wire/sheath structure are a kind of potentially useful 1D nanostructure. Recently, some methods have been developed to synthesize nanocables having coaxial structures. For example, Si/SiO_2 nanocables and three-layered nanocables consisting of silicon carbide (SiC) cores, amorphous silica intermediate layers, and sheaths of boron nitride and carbon (BNC) have been prepared by a laser ablation method,[6] and a β-SiC/SiO_2 nanocable has been obtained by a carbothermal reduction method.[7] In addition, several solution-based methods have also been developed to generate polymer/polymer, semiconductor/polymer, and metal/polymer nanocables at relatively low temperatures. For instance, polypyrrole/poly(methyl methacrylate) coaxial nanocables have been synthesized by sequential polymerization of monomers within the channels of mesoporous silica, followed by dissolution of the template.[8] CdSe/poly(vinyl acetate) hybrid nanocables have been obtained by growing the semiconductor nanowires inside polymer tubules.[9] Gold nanorods have recently been coated with polystyrene or silica to form cable-like structures,[10] and layer-by-layer deposition of oppositely charged species on nickel nanorods has been adopted to prepare nickel/composite nanocable structures.[11] Ag/SiO_2 nanocables can be formed by using a sol–gel method to coat Ag nanowires with amorphous silica,[12] and silver/carbon nanocables can be synthesized by a hydrothermal carbonization co-reduction (HCCR) technique.[13] Very recently, a one-step synthesis of silver/cross-linked PVA nanocables by in situ reduction of Ag^+ and Ag^+-catalyzed cross-linking of PVA chains under hydrothermal conditions inspired us to evaluate whether such a simple route can be applied to semiconductor/polymer nanocables.[14] Our experimental results are in good agreement with our expectations.

Based on the above idea and strategy, we successfully synthesized ultralong and uniform semiconductor tellurium/polymer nanocables with a 25–35 nm core and 30–40 nm diameter sheath and lengths of 500–800 μm by a facile hydrothermal reduction process using PVA and Na_2TeO_3 as starting material at relatively low temperature via a solid solution-solid transformation and the synergistic soft–hard template mechanism. Surprisingly, we found that the aspect ratio of the nanocables with semiconductor tellurium as core and polymer as shell is between 10 and 20000, which may stem mainly from their geometry-dependent properties, and may suggest their use as attractive basic building blocks that can be applied in a variety of applications.[15] In addition, an interesting feature of some nanocables is their tendency to entangle with each other to form raft-like cable bundles in a parallel fashion. The mechanism of formation of these tellurium nanostructures is discussed. To the best of our knowledge, the synthesis of flexible tellurium/poly-

[a] Hefei National Laboratory for Physical Sciences at Microscale and Department of Chemistry, University of Science and Technology of China,
Hefei, Anhui, 230026, China
Fax: +86-551-360-7402
E-mail: ytqian@ustc.edu.cn
[b] Department of Chemistry, University of Science and Technology of China,
Hefei, Anhui, 230026, China

mer nanocables has not yet been reported. Meanwhile, this synthetic method may be applied to the fabrication of other semiconductor/polymer nanostructures.

Results and Discussions

The panoramic morphology of tellurium was observed by field-emission scanning electron microscopy (FESEM), in which the solid samples were mounted on a copper mesh without any dispersion treatment. Parts a and b in Figure 1 show that the final product is composed of nanowires in high yields (close to 100%), with lengths up to 500–800 μm and a uniform morphology. Higher magnification FSEM images (Figure 1, b) indicate that the average diameter of an individual nanowire is about 25–35 nm. TEM images (Figure 1, c–e) reveal that all wires are actually a composite comprised of a smooth core about 25–35 nm in diameter and a surrounding sheath about 5–10 nm in thickness, from which the contrast between surrounding polymer and inner core can be easily observed. One can see that the sheath has a relatively uniform thickness over the entire surface of each nanowire, including both ends, as shown in Figure 1 (c–e). FESEM and TEM both demonstrate that some bundles of cables are formed, and each bundle is composed of several nanocables packed in a parallel fashion (Figure 1, b–d). More-detailed TEM observations revealed that the nanocables structures have a closed end, as shown in Figure 1, e. It is clear that the uniformity in lateral dimension, the level of perfection, and the richness in quantity are obviously due to a good growth environment for the tellurium nanostructures in the current system (see part a in Figure 1).

The as-obtained samples were also examined by XRD (Figure 2). All the reflection peaks in a 2θ range from 20° to 70° can be readily identified with the hexagonal phase of tellurium, with calculated lattice parameters a = 4.457 and c = 5.927 Å, which shows good consistency with the reported data (JCPDS 36-1452).

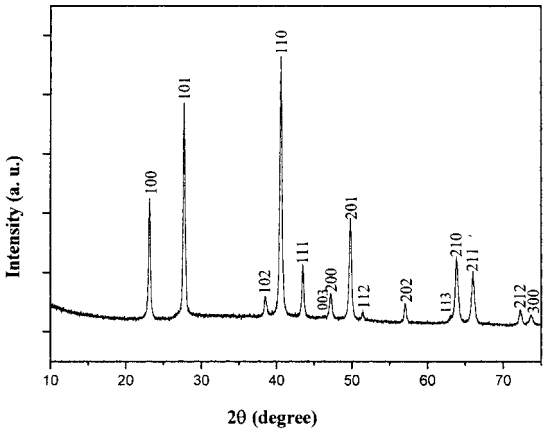

Figure 2. XRD patterns of the nanocables obtained at 180 °C for 24 h.

Further evidence for the surface composition of the samples was obtained from the X-ray photoelectron spectra of the products. The results are shown in Figure 3. The spectra of the nanocables show two strong peaks at 284.60 and 532.10 eV corresponding to the C 1s and O 1s binding energies of the obtained sample, respectively. However, the binding energy at 573.6 and 583.8 eV for Te^0 $3d_{5/2}$ and $3d_{3/2}$, respectively, are quite weak and almost cannot be detected. These XPS results confirm that the tellurium nanowires are confined within shells of the cross-linked PVA. The IR spectrum for the as-obtained nanocables is shown in Figure 4. Several absorption peaks located at about 3449, 2923, and 1461 cm^{-1} in Figure 4 correspond to the O–H stretching vibration [ν(O–H)], the C–H stretching vibration [ν(C–H)], and the C–H bending vibration [δ(C–H)], respectively, as in the IR spectrum of pure PVA, while the wide absorption peak at about 1097 cm^{-1} can be assigned to the ν_{as}(C–O–

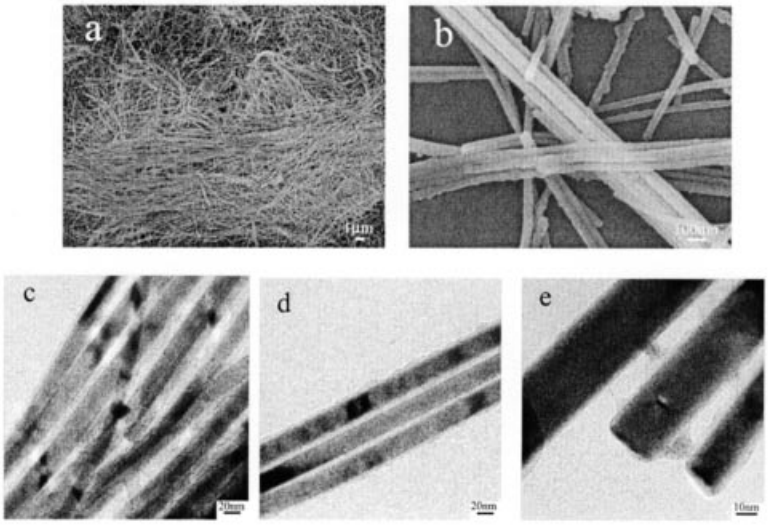

Figure 1. FESEM and TEM images of the nanocables: (a) general view of the cables; (b) magnified FESEM image of the cables; (c–e) TEM images of the cables, clearly revealing the inner core–shell structure.

C) absorption of cross-linked PVA. These results confirm that coating of the tellurium nanowires with cross-linked PVA has been achieved using the current hydrothermal method.

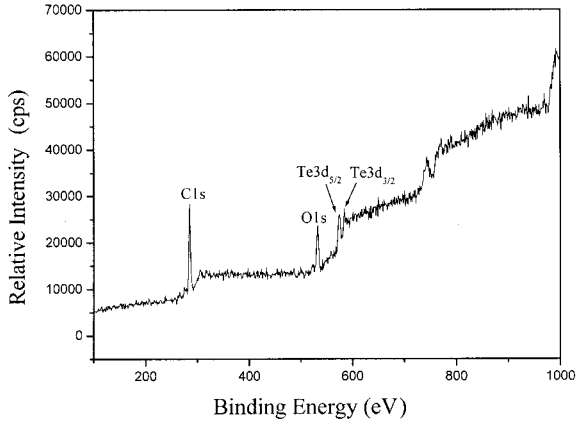

Figure 3. XPS spectrum of the nanocables obtained at 180 °C for 24 h.

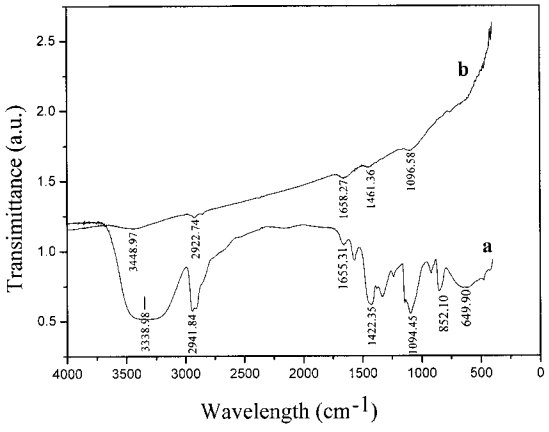

Figure 4. FTIR spectra: (a) pure PVA; (b) the nanocables obtained after reaction at 180 °C for 24 h.

The structure and morphology of the as-obtained nanocables were further observed by high-resolution TEM (HRTEM) and selected-area electron diffraction (SAED), in which the sample was treated by ultrasonic dispersion in ethanol for 15 min and then put onto a copper mesh. Figure 5 (a) shows a typical TEM image of the nanostructures, which confirms that they are composed of a very uniform diameter of the crystalline core surrounded by an amorphous coating. The average diameter of the core of this nanowire is about 25 nm, and the total diameter including the amorphous sheath is about 35 nm. The HRTEM image in Figure 5 (c) recorded from the core tellurium nanowires reveals that the core nanowire shown in the image is about 0.20 nm, which agrees with the (003) lattice planes of t-Te. Figure 5 (b) shows the corresponding ED pattern of the core tellurium nanowires, which was obtained by focusing the electron beam along the [1$\bar{1}$0] zone axis of an individual cable. Moreover, the SAED patterns taken from various regions of the core nanowire are essentially the same. The HRTEM image and ED pattern both demonstrate that the core tellurium nanowire is single-crystalline, with the growth direction along [001]. The perfect diffraction pattern and lattice fringes indicate that the core nanowire is well-crystallized.

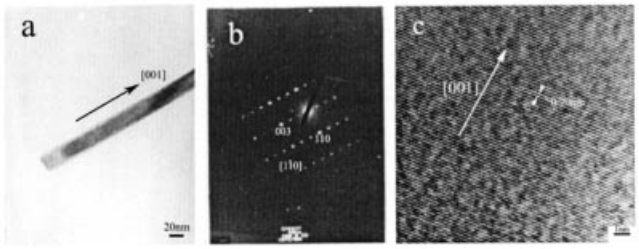

Figure 5. The electron diffraction pattern and HRTEM image of a typical nanocable. HRTEM image (c) taken from the edge of the core tellurium nanowire (a) with growth direction [001], fringe spacing d = 0.2 nm, showing that the core tellurium nanowire is structurally uniform, dislocation free, and single-crystalline. The corresponding ED pattern (b) was obtained from the same tellurium nanostructure, indicating the growth direction and the single-crystalline nature of the core tellurium nanowire.

Further advancement of this approach to nanocables' synthesis requires a clear understanding of the nucleation and growth mechanism. We therefore investigated the evolution of Te nanostructures (taken at the early stages) by TEM. Figure 6 shows the scenarios for the formation of Te nanostructures prepared by the hydrothermal treatment at different times. These images clearly show the evolution of tellurium nanostructures from nanoparticles to nanowires (cables) over time at 180 °C. After heating for 3.5 h, a gray precipitate was formed. The TEM results demonstrated that a large number of irregular nanoparticles with sizes of 10–20 nm and their larger aggregates had formed (Figure 6, a). The SAED patterns (insets of Figure 6, a) clearly reveal that the initial product of the reduction reaction was a mixture of amorphous Te (a-Te) colloids and t-Te nanocrystals. In addition, the colorless solution changed to a yellow-brown color, which implies that PVA has been oxidized by Na_2TeO_3 into cross-linked PVA, which is insoluble in water. After 5 h, the products were composed of a mixture of spherical nanoparticles and a small fraction of nanowires. Figure 6 (b) is a typical TEM image of the sample taken from the solution at this stage. It is clear that these nanowires have diameters of about 30 nm and lengths of several hundreds of nanometers. The ED pattern (insets of Figure 6, b) shows that these nanowires are single crystalline t-Te and that the spherical nanoparticles are composed of a mixture of a-Te and t-Te nanoparticles (marked by arrow). After heating for 8 h, nanowires with diameters of about 30 nm and lengths of up to several micrometers can be distinctly observed (Figure 6, c). In addition, at this stage the products also contain a small quantity of nanparticles (less than 10%). Further extending the heating time led to the formation of ultralong nanowires. Figure 6 (d) is a typical TEM image of a sample prepared after heating for 24 h, indicating that the obtained products are dominated by the ultralong wire-like nanostructures. These nanowires are uni-

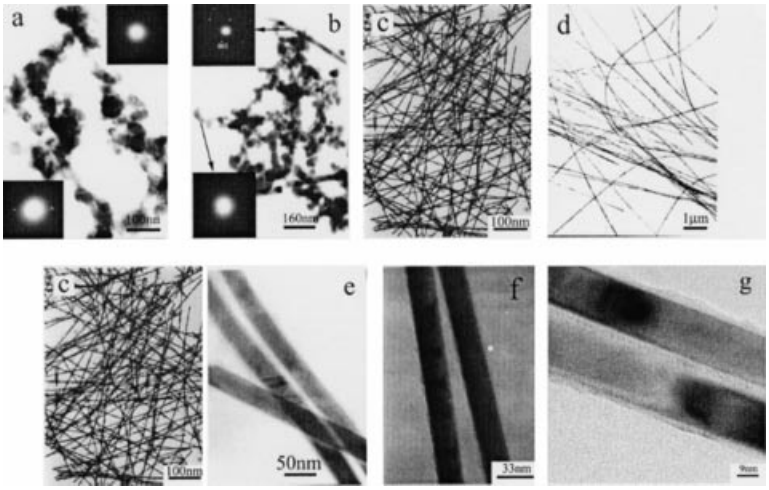

Figure 6. TEM images of Te nanostructures generated by the hydrothermal process after different times: (a) 3.5 h [the insets in Figure 6, part a, show the ED patterns, which indicate that both t-Te (bottom left) and a-Te nanoparticles (upper right) coexist in the initial products]. (b and e) 5 h, a few short nanowires can be observed. (c and f) 8 h and (d and g) 24 h. The insets in Figure 6, part b, are the ED patterns, which reveal that both t-Te nanowires/nanoparticles (upper left) and a-Te nanoparticles (bottom left) coexist in this product (as indicated by arrows).

form in diameter (25–35 nm) and their lengths extend to hundreds of micrometers. From Figure 6 (b–d) one can see that the growth of these nanowires along the longitudinal direction is quite quick, while the growth of their lateral dimensions is very slow and the diameter of nanowires almost does not change during the whole reaction. In addition, one can see that all these nanowires are actually a composite comprised of a core–sheath structure (see Figure 6, e–g), which suggests that the growth of wires and the formation of core–sheath structures occurs simultaneously. Furthermore, the lengths of these nanocables are mainly determined by the original tellurium nanowires and can be as long as several hundreds of micrometers.

As we all know, PVA chains crosslink after treatment at high temperature (250 °C); however, in the absence of Na_2TeO_3, we found that hydrothermal treatment of a PVA solution cannot make it cross-linked at 180 °C or even 200 °C, while the cross-linking reaction occurs at 160–180 °C in the presence of Na_2TeO_3. These results clearly demonstrate that the current hydrothermal process is an efficient method for promoting the cross-linking reaction. In this hydrothermal process, PVA can be oxidized by Na_2TeO_3 at 160–180 °C into cross-linked PVA, which is insoluble in water. As a result, the presence of Na_2TeO_3 is essential for the formation of cross-linked PVA and the formation of cables. In addition, when PVA was not added to the reaction system, we found that the reaction could not be initiated at all. In fact, PVA could serve as both reducing reagent and capping reagent in the present synthesis. Na_2TeO_3 can be reduced by PVA at 180 °C into tellurium nanoparticles and further grow into nanowires with the assistance of PVA; in turn, the tellurium nanowires serve as a hard template on which the core–sheath structures will form. It is reasonable to assume that, under the present hydrothermal conditions, the formation of the hybrid nanostructures is by synergistic growth, as both the growth of wires and the formation of core–sheath structures occur at the same time and are tightly linked to each other. The good agreement between the experimental data and our expectations suggests that it should be possible to rationally choose appropriate reaction

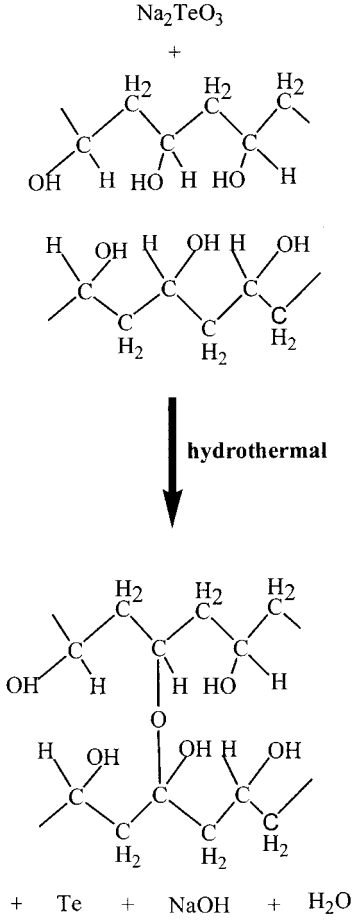

Scheme 1.

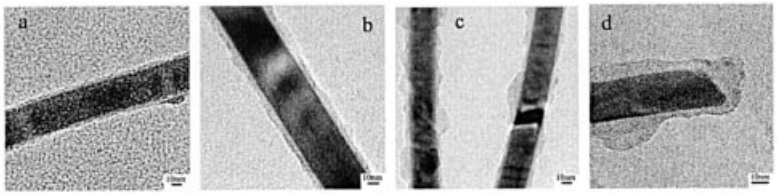

Figure 7. TEM images of tellurium/PVA coaxial nanocables obtained after the coating reaction had processed for (a) 8, (b) 24, (c) 36, and (d) 48 h, clearly showing that the thickness of the sheath increases from 2 to 10–20 nm.

systems for the synthesis of nanocables. In addition, it is worth pointing out that the pH value remains almost the same (10.40 for the starting initial solution to 9.42 for the residual solution) during reaction, thus suggesting that the solution after reaction is still more basic. According to the above results, the reaction that occurs under the current hydrothermal conditions can be formulated as shown in Scheme 1.

The final morphology of the tellurium nanostructures synthesized by the hydrothermal process is highly reliant on the amount of PVA added to the reaction solution. A number of experiments were performed with a procedure similar to that mentioned in the Experimental Section, and we found that the amount of PVA was crucial for the formation of nanocables, with the amount of PVA (5 mL) being suitable for the formation of cables. When the amount of PVA was relatively high (10 mL), no cables and only short tellurium nanorods were obtained as the final products (data not shown). The absence of nanowires (or cables) in the final product could be attributed to the high concentration of PVA, which might lead to the formation of a thick coating over the surface of the nanoparticles. Therefore, the selectivity of the interaction between PVA and various crystallographic planes is weakened, and anisotropic growth can essentially not be induced.

The thickness of the sheath can also be controlled by changing the reaction time. Figure 7 (a–d) show a set of TEM images of the cables that were obtained after different periods of time, and reveal that the thickness of the sheath can be increased by up to 10–20 nm by increasing the reaction time to 48 h. In addition, the amount of PVA and concentration of Na_2TeO_3 also play a key role in the formation of tellurium nanostructures. The reaction of Na_2TeO_3 (2 mmol) with less PVA (1 mL), with the other conditions remaining the same, gives only tellurium nanoparticles; no nanocables were observed. Moreover, if less Na_2TeO_3 (0.5 mmol) was used, with the other conditions remaining unchanged, no cables were obtained.

On the basis of the above results, we propose that the formation of tellurium nanocables follows the PVA-assisted solid solution-solid (SSS) transformation and the synergistic soft–hard template (SSHT) mechanism. It is clear that PVA is responsible for both the formation of tellurium nanoparticles and the subsequent oriented growth of tellurium nanowires. Firstly, the a-Te and t-Te nanoparticles a produced by the reduction of TeO_3^{2-} by PVA at 180 °C. The colloids of a-Te would dissolve into the solution due to their higher free energies than those of t-Te nanocrystals. This dissolved Te (at the expense of a-Te) colloid subsequentlyforms crystalline nanowires on the seeds of t-Te due to the assistant of PVA and the anisotropic nature along the [001] direction.[16] In turn, the tellurium wires serve as a template on which cross-linked PVA forms. In addition, the newly formed cross-linked PVA will act as an effective bridge to connect nearby single cables to form raft-like cable bundles in a parallel fashion. It is worth mentioning that the growth of nanowires and the formation of core–sheath structures occur at the same time (see Figure 6, e–g).

Conclusions

In conclusion, we have demonstrated a facile hydrothermal synthesis of ultralong nanocables with tellurium as cores and cross-linked PVA as sheaths in high yield. In the present system, the synergistic actions of both the stabilization of PVA and the binding interaction of cross-linked PVA with the tellurium nanowires could play a key role in the formation of the morphology of the resulting products. The current elegant nanocables with a high aspect ratio may have potential technological applications in nanoscience and nanotechnology. Meanwhile, we believe that the present convenient method could be extended to prepare other semiconductor/polymer or metal/polymer coaxial cables by an appropriate choice of reaction system and experimental conditions. Further work in this area is in progress.

Experimental Section

Synthesis: In a typical experimental procedure, analytically pure Na_2TeO_3 (2 mmol) and 5 mL of PVA (5 wt.-%) solution were put into 40 mL of distilled water at room temperature to form a clear solution, which was then stirred strongly for about 0.5 h and transferred into a 50-mL Teflon-lined stainless-steel autoclave. The autoclave was sealed and maintained at 180 °C for 24 or 48 h and then air-cooled to room temperature naturally. A large quantity of black-gray, wire-like flocculent material was found floating on the top of the solution. This material was collected and washed with distilled water and anhydrous alcohol several times to remove ions and possible remnants in the final product. It was then dried in a vacuum oven at 60 °C for 4 h.

Characterization: The X-ray powder diffraction (XRD) analysis was performed with a Japanese Rigaku D/max-γA rotating anode X-ray diffractometer equipped with monochromatic, high-intensity Cu-K_α radiation (λ = 1.54178). The X-ray photoelectron spectra (XPS) were collected on an ESCALab MKII X-ray photoelectron

spectrometer, using nonmonochromatized Mg-K_α X-rays as the excitation source. Field emission scanning electron microscope (FESEM) images were taken on a JEOL JSM-6300F SEM. Transmission electron microscopy and electron diffraction (ED) patterns were taken with a Hitachi Model H-800 instrument using an accelerating voltage of 200 kV with a tungsten filament. TEM and high-resolution TEM (HRTEM) were obtained on a JEOL-2010 transmission electron microscope at an acceleration voltage of 200 kV. Infrared (IR) analysis of the precursor was conducted on a Magna IR-750FT Spectrometer ranging from 400 to 4000 cm^{-1} at room temperature with the samples mulled in KBr wafer.

Acknowledgments

The financial support of this work by the National Natural Science Foundation of China, the 973 Project of China, and a State Key Project of fundamental research of nanomaterials and nanostructures, is gratefully acknowledged.

[1] F. Caruso, *Adv. Mater.* **2001**, *13*, 11–22.
[2] Y. Xia, B. Gates, Y. D. Yin, Y. Lu, *Adv. Mater.* **2000**, *12*, 693–713.
[3] J. J. Schneider, *Adv. Mater.* **2001**, *13*, 529–533.
[4] W. Schärtl, *Adv. Mater.* **2000**, *12*, 1899–1908.
[5] C. J. Kiely, J. Fink, J. G. Zheng, M. Brust, D. Bethell, D. J. Schiffrin, *Adv. Mater.* **2000**, *12*, 640–643.
[6] A. M. Morales, C. M. Lieber, *Science* **1998**, *279*, 208–211.
[7] a) G. W. Meng, L. D. Zhang, C. M. Mo, S. Y. Zhang, Y. Qin, S. P. Feng, H. J. Li, *J. Mater. Res.* **1998**, *13*, 2533–2538; b) L. D. Zhang, G. W. Meng, F. Phillipp, *Mater. Sci. Eng. A* **2000**, *286*, 34–38.
[8] J. Jang, B. Lim, J. Lee, T. Hycon, *Chem. Commun.* **2001**, 83–84.
[9] Y. Xie, Z. Qiao, M. Chen, X. Liu, Y. Qian, *Adv. Mater.* **1999**, *11*, 1512–1515.
[10] S. O. Obare, N. R. Jana, C. J. Murphy, *Nano Lett.* **2001**, *1*, 601–603.
[11] K. S. Mayya, D. I. Gittins, A. M. Dibaj, F. Caruso, *Nano Lett.* **2001**, *1*, 727–730.
[12] Y. Yin, Y. Lu, Y. Sun, Y. Xia, *Nano Lett.* **2002**, *2*, 427–430.
[13] S. H. Yu, X. J. Cui, L. Li, K. Li, B. Yu, M. Antonietti, H. Cölfen, *Adv. Mater.* **2004**, *16*, 1636–1640.
[14] L. B. Luo, S. H. Yu, H. S. Qian, T. Zhou, *J. Am. Chem. Soc.* **2005**, *127*, 2822–2823.
[15] a) P. M. Ajayan, *Chem. Rev.* **1999**, *99*, 1787–1800; b) S. Link, M. A. El-Sayed, *J. Phys. Chem. B* **1999**, *103*, 8410–8426; c) Y. Zhang, K. Suenaga, C. Colliex, S. Iijima, *Science* **1998**, *281*, 973–975.
[16] L. Berg, V. Haase, I. Hinz, G. Kirschstein, H. J. Richter-Ditten, J. Wagner, *Gmelin Handbook of Inorganic Chemistry* (Eds.: G. Czack, D. Koschel, H. K. Kugler), Springer-Verlag, Berlin, **1983**, vol. 8, pp. 1–223.

Received: July 23, 2005
Published Online: November 17, 2005

